

A dc-coupled, HBT-based transimpedance amplifier for the LISA quadrant photoreceivers

Germán Fernández Barranco and Gerhard Heinzl

Abstract

The quadrant photoreceivers (QPRs) in the Laser Interferometer Space Antenna (LISA) mission must feature an input-referred current noise below $2 \text{ pA Hz}^{-1/2}$ at 25 MHz to avoid degradation of the signal-to-noise ratio. We present a QPR with a dc-coupled transimpedance amplifier (TIA) based on heterojunction bipolar transistors (HBTs). The QPR features an input-referred current noise density below $1.5 \text{ pA Hz}^{-1/2}$ at 25 MHz, a 37 MHz bandwidth and a 56.2 mW power consumption. Additionally, the dc-coupled, HBT-based TIA allows the QPR to fulfill the size and interface requirements of the LISA mission.

Index Terms

photoreceiver, transimpedance amplifier, heterodyne laser interferometry, intersatellite metrology, gravitational waves, geodesy.

I. INTRODUCTION

A quadrant photoreceiver (QPR) is the combination of a 4-segment quadrant photodiode (QPD) and 4 transimpedance amplifiers (TIAs). The QPR is a key component in intersatellite laser interferometers, where very weak MHz optical signals must be detected. In the Laser Interferometer Space Antenna (LISA) [1], the μW laser beam in the local spacecraft interferes with an incoming pW laser beam arriving from the distant spacecraft. This interference produces a MHz beat-note of the order of nW . QPRs must convert the MHz (also known as rf) optical beat-note into a voltage without introducing excessive phase noise. The beat-note phase contains the

(Corresponding Author: Germán Fernández Barranco)

G. Fernández Barranco and G. Heinzl are with the Max Planck Institute for Gravitational Physics (Albert Einstein Institute), 30167 Hannover, Germany, and also with the Institut für Gravitationsphysik, Leibniz Universität Hannover, 30167 Hannover, Germany (e-mail: german.fernandez.barranco@aei.mpg.de).

angular and longitudinal displacements intended to be measured with the laser interferometer. QPR contributions to the overall phase noise have been studied in [2], [3]. In this work, we focus on the contribution from the photoreceiver input-referred current noise density or \tilde{i}_{en} .

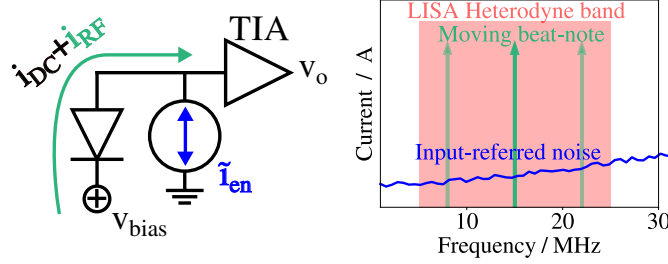


Fig. 1. Signal versus amplitude noise in the LISA quadrant photoreceiver (QPR). On the left, a simplified circuit diagram of the QPR showing the quadrant photodiode (QPD) segment and photocurrent, the transimpedance amplifier (TIA) and the input-referred current noise source. On the right, the spectral picture (not scaled) showing the main rf signal (green) and the noise (blue). The noise is usually given in $A Hz^{-1/2}$. The rf signal has a variable frequency within the LISA heterodyne band, from 5 MHz to 25 MHz. The signal-to-noise ratio worsens towards higher frequencies.

Figure 1 graphically shows the contribution from \tilde{i}_{en} . A segment of the QPD detects the optical signal and generates a photocurrent. The photocurrent has a μA dc component and the critical nA rf component. The rf component (green in Figure 1) has a varying frequency within the LISA heterodyne range, from 5 MHz to 25 MHz. A TIA is used to convert the photocurrent into a voltage. The voltage signal is sent to the subsequent units of the metrology chain via coaxial cables. The QPR has intrinsic electronic noise that can be modeled as a current source at the TIA input: the input-referred current noise or \tilde{i}_{en} (blue in Figure 1). The value of \tilde{i}_{en} is not only influenced by the TIA voltage noise \tilde{e}_n and TIA current noise \tilde{i}_n but also by the junction capacitance C_J of the QPD segment. A simplified relation is

$$\tilde{i}_{en} \propto (\tilde{i}_n^2 + (\tilde{e}_n C_J f)^2)^{1/2}, \quad (1)$$

$$[\tilde{i}_{en}] = A Hz^{-1/2},$$

where f is the frequency and several less-relevant parameters were omitted. The contribution from C_J and the TIA voltage noise \tilde{e}_n dominates \tilde{i}_{en} at high frequencies, including the LISA heterodyne band. The spectral picture on the right-hand side of Figure 1 describes the aforementioned scenario, where the signal-to-noise ratio decreases towards higher frequencies.

Describing how the signal-to-noise ratio converts into interferometer phase noise is out of the scope of this work. A detailed description of this relation can be found in [4, p. 45]. From

the QPR perspective, an input-referred current noise \tilde{i}_{en} below $2 \text{ pA Hz}^{-1/2}$ up to 25 MHz is considered acceptable and would not cause a significant degradation of the LISA interferometer performance.

Other key parameters of the LISA QPRs are power consumption and size. Figure 2 shows a preliminary concept of the LISA optical bench, where all 12 QPRs have been highlighted. The high number of QPR units on the densely populated, 450-mm-diameter optical bench imposes restrictions on the QPR size. This preliminary optical bench concept assumes a TIA PCB size below $49 \text{ mm} \times 53.2 \text{ mm}$ to comply with the allocated volume. Additionally, the required thermal stability to achieve pm precision in the interferometer demands low power consumption and low heat dissipation from all active components on the optical bench. The current baseline limits the power consumption for each QPR to 200 mW.

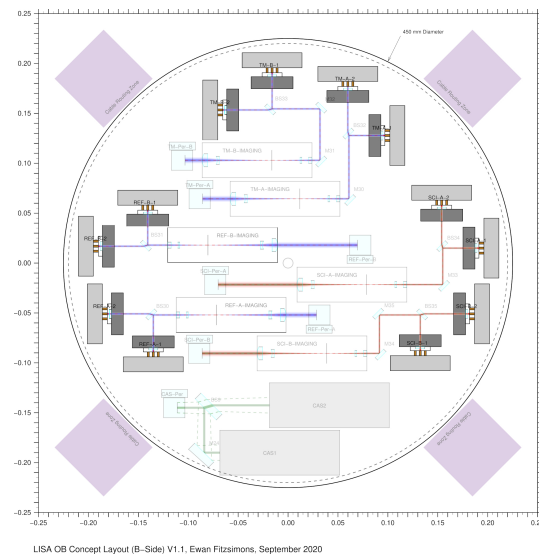


Fig. 2. Preliminary concept of the LISA optical bench (B-Side). The figure highlights all 12 QPRs, which are placed on the outer edge of a densely populated, 450-mm-diameter bench. The tight layout sets stringent constraints on the QPR size. Additionally, the overall power consumption must be low to reach the high thermal stability needed for picometer-precision interferometry. Image credit: UK Astronomy Technology Center and University of Glasgow.

Previous efforts towards a LISA-like QPR focused mainly on the input-referred current noise \tilde{i}_{en} and bandwidth. Discovery Semiconductors Inc. developed custom QPDs with a very low C_J ($\sim 12.7 \text{ pF mm}^{-2}$). The custom QPDs have passed preliminary space qualification [5]. A low-capacitance ($C_J = 2.5 \text{ pF}$), 1-mm-diameter QPD was tested in combination with an OpAmp-based TIA (EL5135), showing an input-referred current noise below $1.9 \text{ pA Hz}^{-1/2}$ at 25 MHz and a

3 dB bandwidth of ~ 20 MHz, below the maximum LISA heterodyne frequency of 25 MHz. Noise and bandwidth were limited by the OpAmp used in the TIA.

The authors of this work designed a TIA based on heterojunction bipolar transistors (HBTs) to overcome the limitations of OpAmp-only TIAs. The proof-of-concept prototype featured an input-referred current noise below $1.9 \text{ pA Hz}^{-1/2}$ at 25 MHz and a 3 dB bandwidth of ~ 37 MHz, when tested with a $C_J \sim 3.8 \text{ pF}$ [6]. While these results showed the potential of an HBT-based TIA, the prototype did not meet the specifications of a LISA QPR in terms of size, power consumption, space-qualified components and number of interfaces.

The QPR Working Group (QPRWG) was established within the frame of the LISA Consortium to develop QPRs which fulfill all requirements for the LISA mission and to coordinate the activities with other LISA subsystems groups. The QPRWG is an international collaboration with members in Belgium, France, Germany, Japan [7], the Netherlands and the United Kingdom. The authors of this work, now as members of the QPRWG, focused their efforts on correcting various shortcomings of the proof-of-concept HBT-based TIA.

Hereby we present a TIA design featuring HBTs and a dc-coupled topology. The dc-coupled topology requires less components, which decreases the QPR size, input-referred current noise and power consumption. Additionally, the number of signal lines halves with respect to the rf-dc split topology from [6], which is critical for the QPR housing and harness. The TIA components have been carefully selected, using devices with space-qualified counterparts or that were previously used in space missions. A detailed description of the dc-coupled, HBT-based TIA is presented in Section II. The experimental characterization of Section III shows how the dc-coupled, HBT-based TIA outperforms previous TIA-topologies. Based on these results, the dc-coupled, HBT-based TIA is a strong candidate for the LISA QPR flight models.

II. DESIGN DESCRIPTION

The motivation for this work was to replace the rf-dc split TIA from [6] with a dc-coupled configuration. In [6], the rf component of the photocurrent was amplified at an HBT-based, rf-only stage. The dc component had a dedicated OpAmp-only stage. Figure 3 shows the circuit diagram of the dc-coupled, HBT-based TIA. The operating principle is similar to the rf-only section of [6].

The cascode: the photocurrent is first amplified at an ultra-low noise, HBT-based cascode stage. As in the rf-dc split TIA, the use of HBTs for the critical initial amplification is motivated

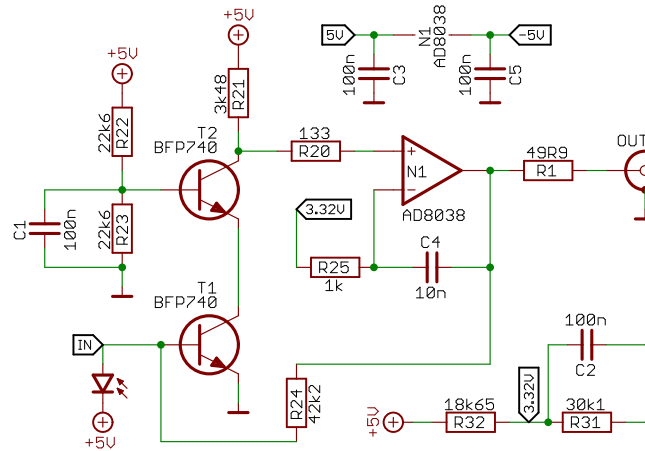


Fig. 3. Circuit diagram of the TIA for one QPR channel. The key point of this design is the single, dc-coupled TIA topology. A low noise heterojunction bipolar transistor (HBT) with a space-qualified equivalent, the BFP740, is used in a common emitter, cascode configuration. An additional low power non-inverting amplifier is used to maintain the bandwidth and increase the gain. After combining the previously separated dc and rf paths [6], the TIA requires less components and features lower noise and a lower power consumption, as shown in Section III.

by the lower noise of these devices compared to OpAmps. An in-depth explanation of the HBT parameters that affect the noise can be found in [6]. The transistor model was changed from the BFP842ESD to the BFP740, which is also an HBT from Infineon Technologies based on SiGe:C [8]. The BFP740 was especially chosen due to its similarity to a space-qualified HBT, the BFY740B-01 [9]. The cascode topology with two HBTs reduces the Miller effect and maintains the bandwidth [10]. The amplification factor of the cascode stage is given by the current gain of the BFP740. For a collector current I_C of 0.48 mA, as for the dc-coupled TIA, the BFP740 current gain is ~ 390 . The collector current I_C is a critical parameter which defines not only the current gain but in general the noise, bandwidth and power consumption of the TIA [6].

The non-inverting amplifier: the signal is further amplified in an OpAmp-based stage. This OpAmp also provides a low impedance path to ground at the output of the TIA. As in [6], the AD8038 from Analog Devices was chosen for this OpAmp-based stage due to its high bandwidth and low power consumption. The difference with respect to the AD8038 from [6] is the package: a small SC70 was used instead of the standard SOIC-8. The SC70 package has obvious benefits for the total TIA size. The AD8038 also has space heritage. It is used in two space missions still in operation; CASSIOPE from the Canadian Space Agency [11] and TESS from NASA. NASA successfully tested the AD8038 SC70 response to destructive single event failure [12], and only

a Total Ionizing Dose test might be required to qualify the AD8038 SC70 for the LISA mission.

Resistor R24 connects the TIA input and output, providing negative feedback and setting the transimpedance gain ($G_{\text{TIA}} = 42.2 \text{ k}\Omega$).

The main challenge of the dc-coupled, HBT-based TIA was its biasing. In the rf-dc split TIA [6], a set of ac-coupling capacitors provided flexibility to adjust the operating point of the different stages independently. The biasing of the input HBT, the cascode collector current I_C and the OpAmp bias could all be easily set with the corresponding resistors, without affecting other sections of the circuit. For the dc-coupled TIA, where all ac-coupling capacitors were removed, two major modifications were needed to provide the required biasing:

- A dc voltage of 3.32 V is used at N1's inverting input with the purpose of fixing T2's collector voltage, which in turn sets the cascode collector current I_C . A resistor voltage divider (R31 and R32) produces the 3.32 V from the 5 V positive supply.
- The feedback resistor across the non-inverting amplifier (N1 OpAmp) was removed. A resistor in N1's feedback path allows the dc output voltage to influence N1's inputs, which in turn affects the critical cascode collector current I_C . The feedback capacitor C4 and resistor R25 set the frequency response of the OpAmp stage.

With aforementioned adjustments, the dc photocurrent level at the input affects only the dc output voltage. In other words, the TIA operating point is fixed by the overall negative feedback topology of the TIA. This also implies that the input HBT (T1) does not require an emitter or base biasing resistors. The suppression of resistors at the input stage has a positive impact on the noise, since all resistors feature thermal (Johnson-Nyquist) noise. The dc output voltage is equal to T1's base-emitter voltage ($\sim 0.71 \text{ V}$) for no input photocurrent, and decreases with increasing photocurrent.

The 133Ω resistor R20 was originally used in a low-pass filter at N1's non-inverting input. The low-pass filter was discarded during the prototyping process, but R20 was found useful to mitigate oscillations that occurred when there was a direct connection between T2 and N1.

Figure 4 shows the PCB layout of the QPR prototype featuring the dc-coupled, HBT-based TIA. There are four TIAs in total on the QPR, one per QPD segment. Two TIAs are located on the top layer and two on the bottom layer. Previous HBT-based TIA designs featured all channels on the same layer. The stringent size constraints for the LISA QPRs motivated the current topology, which only requires half of the area for the TIAs. There was a concern about overlapping TIAs interfering with each other and leading to oscillatory behavior. However, the

experimental characterization of the prototype (Section III) does not indicate any degradation in performance due to this topology. The 2 inner layers of the 4-layer PCB are used for power supply distribution and a ground plane. Cutouts on the ground plane were performed along the signal path to reduce potential parasitic effects.

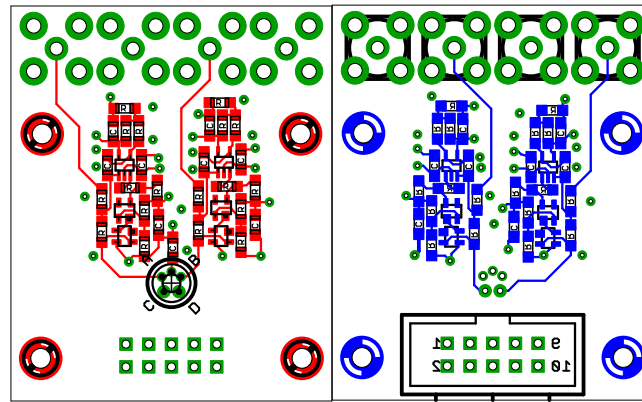


Fig. 4. PCB layout of the top (left) and bottom (right) layers of the QPR prototype. Two TIAs featuring the topology shown in Figure 3 are located on each side. The PCB size is 36 mm x 44 mm, greatly influenced by the type of connectors used. Further iterations of the design will feature smaller, space-qualified connectors. The inner layers of the 4-layer PCB are used for power supply distribution and ground. Each of the four channels has its own supply lines. Cutouts on the ground plane under the signal path were performed to avoid parasitic effects.

Each TIA output has a dedicated SMA connector (four in total). A 10-pin IDC connector is used for the power supply. Two power supply lines (± 5 V) are used by each of the four TIAs. Redundancy schemes of the LISA mission require individual TIA power supply control. The bias voltage for the QPD has also a dedicated 5 V line. The PCB size is 36 mm x 44 mm, ~ 5 times smaller than the PCB from [6]. Future QPR iterations featuring space-qualified connectors, such as Nano-D for the power supply, are expected to be even smaller.

Figure 5 shows the top side of one of the implemented QPR prototypes. Two TIAs as well as the QPD are visible. The QPD is an InGaAs, 0.5-mm-diameter detector from OEC GmbH / GPD Optoelectronics Corp. The QPD pins, about 14 mm long, were not directly soldered to the PCB but inserted into pre-soldered sockets. The resistors and capacitors used are standard 0806 SMD passive components.

Passive components were often replaced during prototype debugging. It was observed that the BFP740 and AD8038 SC70 were frequently damaged by resoldering and excess heat. The damage sometimes affected the dc operating point, preventing the QPR from functioning. But

at other times, the QPR continued operating and the damage would only manifest itself as small oscillations at the TIA output. Before the influence of excess heat on the active components was verified, the small oscillations were wrongly attributed to parasitic effects or component values, complicating debugging and optimization significantly.

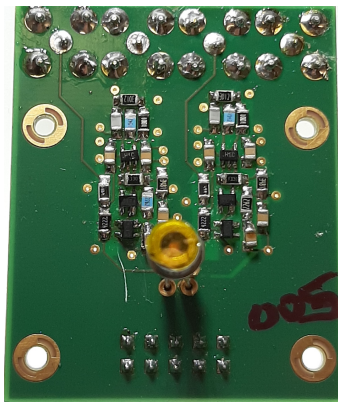


Fig. 5. Picture of the top side of the QPR featuring an InGaAs, 0.5-mm-diameter QPD (GAP5000Q by OEC GmbH / GPD Optoelectronics Corp). The QPD pins were inserted into pre-soldered sockets. The resistors and capacitors are standard 0806 SMD. Passive components were often replaced during prototype debugging. It was observed that the BFP740 and AD8038 SC70 active components were frequently damaged by resoldering and excess heat.

III. EXPERIMENTAL CHARACTERIZATION

The performance of the dc-coupled, HBT-based TIA was measured using the white light method, as in previous publications [6] [13]. A detailed description of the white light method can be found in [3, p. 79]. With this method, one can measure the input-referred current noise and the magnitude of the TIA gain simultaneously. It only requires the use of a shot-noise-limited (hence white) light source, such as a simple halogen bulb. All four TIAs from five QPR prototypes were characterized using this technique, showing a similar performance. For the sake of clarity, only results from a representative TIA are presented.

Figure 6 shows the input-referred current noise \tilde{i}_{en} and the TIA gain G_{TIA} for two InGaAs QPDs of different diameter: the GAP500Q (0.5-mm-diameter) and the GAP1000Q (1-mm-diameter), both from OEC GmbH / GPD Optoelectronics Corp. The use of two devices with different diameters allows us to study the TIA performance versus C_J , the QPD junction capacitance. Figure 6 shows only a representative case.

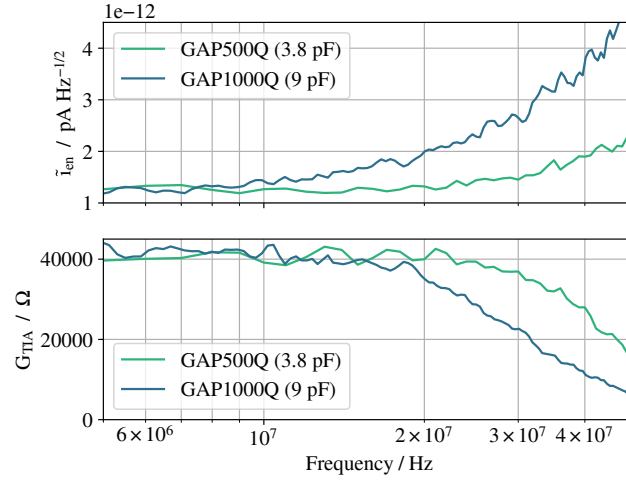


Fig. 6. Input-referred current noise \tilde{i}_{en} and transimpedance gain G_{TIA} of the dc-coupled, HBT-based TIA for two QPD models, both with a 5 V bias voltage. Using the GAP500Q ($C_J = 3.8$ pF), \tilde{i}_{en} is lower than $1.5 \text{ pA Hz}^{-1/2}$ at 25 MHz. The 3 dB bandwidth is approximately 37 MHz. When using the GAP1000Q ($C_J = 9$ pF), \tilde{i}_{en} is lower than $2.5 \text{ pA Hz}^{-1/2}$ at 25 MHz. The 3 dB bandwidth is approximately 24 MHz.

For the GAP500Q, which features a C_J per segment of 3.8 pF, \tilde{i}_{en} is lower than $1.5 \text{ pA Hz}^{-1/2}$ at 25 MHz. The 3 dB bandwidth is approximately 37 MHz. When using the GAP1000Q, a QPD with a C_J per segment of 9 pF, \tilde{i}_{en} is lower than $2.5 \text{ pA Hz}^{-1/2}$ at 25 MHz. The 3 dB bandwidth is approximately 24 MHz.

Figure 7 shows a comparison of the measured input-referred current noise density \tilde{i}_{en} for the two previous TIA topologies proposed for LISA and the dc-coupled, HBT-based TIA presented in this work. The QPD used for all three measurements was the GAP500Q by OEC GmbH / GPD Optoelectronics Corp. The results can be directly compared due to the very similar junction capacitance C_J .

Figure 7 shows the improvement in noise achieved with the dc-coupled, HBT-based TIA. The OpAmp-based solution [13], which featured an ultra-low noise, high-bandwidth OpAmp (EL5135) showed an \tilde{i}_{en} of $2.1 \text{ pA Hz}^{-1/2}$ at 25 MHz. The proof-of-concept HBT-based design [6] presented an \tilde{i}_{en} of $1.9 \text{ pA Hz}^{-1/2}$ at 25 MHz, improving the noise performance at high frequencies. On the other hand, the \tilde{i}_{en} below 18 MHz was worse than in [13]. The dc-coupled, HBT-based TIA improves \tilde{i}_{en} at all frequencies within the LISA heterodyne band, and \tilde{i}_{en} stays below $1.5 \text{ pA Hz}^{-1/2}$ at 25 MHz.

The measured QPR supply current was 7 mA (5 V) and 4.2 mA (-5 V). The power con-

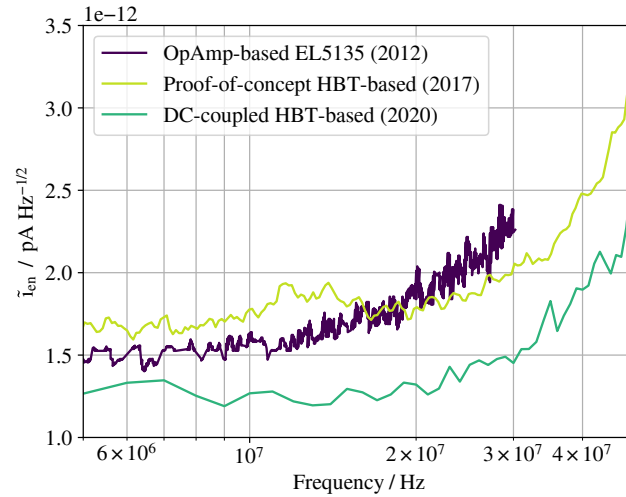


Fig. 7. Comparison of the input-referred current noise \tilde{i}_{en} for three TIA solutions. All 3 cases feature the same QPD, the GAP500Q ($C_J \sim 3.8$ pF). A standard OpAmp-based solution (EL5135) was used in [13], and it showed an \tilde{i}_{en} of $2.1 \text{ pA Hz}^{-1/2}$ at 25 MHz. The proof-of-concept HBT-based solution from [6] showed an \tilde{i}_{en} of $1.9 \text{ pA Hz}^{-1/2}$ at 25 MHz. Finally, the novel dc-coupled, HBT-based TIA features an \tilde{i}_{en} below $1.5 \text{ pA Hz}^{-1/2}$ at 25 MHz and also a lower noise floor at lower heterodyne frequencies.

sumption obtained from these values is 56.2 mW , about three times lower than the 178 mW of the QPR with the rf-dc split, HBT-based TIA [6] and substantially below the current LISA requirement of 200 mW . The suppression of the dc-only stage and the use of a lower collector current for the cascode ($I_C \sim 0.48 \text{ mA}$) explain the improvement in power consumption.

IV. CONCLUSIONS

We have developed and characterized a transimpedance amplifier (TIA) for use in the quadrant photoreceivers (QPRs) of the Laser Interferometer Space Antenna (LISA). The TIA is based on heterojunction bipolar transistors (HBTs) and a dc-coupled topology. The dc-coupled, HBT-based design is built upon a proof-of-concept prototype [6]. The proof-of-concept design was significantly modified to fulfill previously unmet requirements of size, power consumption and number of interfaces. As a result, the previously separated rf and dc stages from [6] were merged in a single, dc-coupled, HBT-based TIA.

This translated to a QPR-PCB size of $36 \text{ mm} \times 44 \text{ mm}$ (80% reduction), a power consumption of 56.2 mW (66.7% reduction) and half the number of outputs. Additionally, the dc-coupled, HBT-based TIA features an input-referred current noise \tilde{i}_{en} lower than any previous QPR TIA.

The input-referred current noise stays below $1.5 \text{ pA Hz}^{-1/2}$ at 25 MHz (maximum LISA frequency) when using a 0.5-mm-diameter InGaAs QPD ($C_J \sim 3.8 \text{ pF}$). The $\sim 37 \text{ MHz}$ 3 dB bandwidth meets the LISA requirement but presents no significant improvement with respect to the proof-of-concept HBT-based TIA.

The active components of the TIA were chosen due to their space heritage (AD8038 SC70) or similarity to space-qualified components (BFP740). This should simplify the qualification of the design for aerospace applications. Also for this purpose, future evaluations include thermal-vacuum and radiation testing. A full performance test, combining the TIA with the rest of the LISA metrology chain, is also planned.

The results presented in this work consolidate the dc-coupled, HBT-based TIA as a strong candidate for the LISA QPRs.

V. ACKNOWLEDGMENTS

This work was supported by the Deutsches Zentrum für Luft- und Raumfahrt (DLR) with funding from the Bundesministerium für Wirtschaft und Technologie (Project Ref. Number FKZ 50 OQ 1801, based on work done under Project Ref. Number FKZ 50 OQ 1301 and FKZ 50 OQ 0601 as well as partly by the Bundesministerium für Bildung und Forschung under FKZ 03F0654B).

REFERENCES

- [1] LISA Consortium, “Laser Interferometer Space Antenna. A proposal in response to the ESA call for L3 mission concepts.” 2017.
- [2] G. Fernández Barranco *et al.*, “Phase stability of photoreceivers in intersatellite laser interferometers,” *Opt. Express*, vol. 25, no. 7, pp. 7999–8010, 2017. doi: 10.1364/OE.25.007999.
- [3] G. Fernández Barranco, “Photodetection in intersatellite laser interferometers,” *Ph.D. Thesis, Gottfried Wilhelm Leibniz Universität Hannover*, 2018.
- [4] O. Gerberding, “Phase readout for satellite interferometry,” *Ph.D. Thesis, Gottfried Wilhelm Leibniz Universität Hannover*, 2014.
- [5] A. M. Joshi *et al.*, “Comprehensive radiation testing of uncooled, free space coupled, ingaas quad photoreceivers,” in *Free-Space Laser Communications XXXII*, vol. 11272. International Society for Optics and Photonics, 2020, p. 112720G.
- [6] G. Fernández Barranco *et al.*, “A low-power, low-noise 37-MHz photoreceiver for intersatellite laser interferometers using discrete heterojunction bipolar transistors,” *IEEE Sensors Journal*, vol. 18, no. 18, pp. 7414–7420, 2018. doi: 10.1109/JSEN.2018.2857202
- [7] K. Izumi *et al.*, “The current status of contribution activities in japan for lisa,” *Progress of Theoretical and Experimental Physics*, 2020.
- [8] Infineon Technologies, “BFP740 Datasheet. SiGe:C NPN RF bipolar transistor,” *Datasheet*, 2018.

- [9] —, “BFY740B-01 Datasheet. HiRel NPN Silicon Germanium RF Transistor,” *Datasheet*, 2012.
- [10] P. Horowitz and W. Hill, *The Art of Electronics*. Cambridge university press Cambridge, 2015, vol. 3.
- [11] H. G. James *et al.*, “The e-pop radio receiver instrument on CASSIOPE,” *Space Science Reviews*, vol. 189, no. 1-4, pp. 79–105, 2015.
- [12] M. V. O’Bryan *et al.*, “Compendium of single event effect results from nasa goddard space flight center,” 2016.
- [13] F. Guzmán Cervantes *et al.*, “Characterization of photoreceivers for lisa,” *Classical and Quantum Gravity*, vol. 28, no. 9, p. 094010, 2011.



Germán Fernández Barranco received the M.Eng. degree in electrical engineering and the M.Eng. degree in telecommunications engineering from the University of Granada, Spain, in 2013, and the Dr.-Ing. degree in electrical engineering from Leibniz Universität Hannover in 2017. He is currently a Post-Doctoral Researcher with the Albert Einstein Institute, Hannover. His research interests include the development and characterization of readout electronics for intersatellite laser interferometers, such as the GRACE Follow-On Laser Ranging Interferometer and the Laser Interferometer Space Antenna.



Gerhard Heinzel received the Ph.D. degree in physics from Leibniz Universität Hannover (LUH) and the Max-Planck-Institut für Quantenoptik, Garching. He spent two years in Japan working on the TAMA gravitational wave detector. He is currently the Head of the Space Interferometry Group, Albert Einstein Institute, Hannover, and also a Professor with LUH. His main areas of research are laser interferometers in space for gravitational physics, including Laser Interferometer Space Antenna (LISA) Pathfinder, the Laser Ranging Interferometer on GRACE Follow-On, and LISA.